Journal of Modeling & Simulation in Electrical & Electronics Engineering Vol 5 (3). 1-9.

Semnan University

*Journal of Modeling & Simulation in Electrical & Electronics Engineering (MSEEE)*

Journal homepage: https://mseee.semnan.ac.ir/

ISSN: 2821-0786

# Determining the Intensity and Occurrence Location of Faults in Transformers using Frequency Response Analysis (FRA) with Novel Multistage Optimization Algorithm and SVMD Decomposition Technique

Siavash Jamshidi[1] and Zahra Moravej[2•]

***Abstract* - Frequency response analysis (FRA) has become a worldwide accepted technique for detecting winding and core deformation in transformers. The main weakness of this technique is its reliance on the level of expertise and experience of personnel and the lack of standards and automatic codes. It is necessary to create reliable FRA interpretation codes for the high-frequency transformer model that can implement the frequency characteristics of real transformers in a wide frequency range. This paper presents an artificial intelligence method to estimate these parameters from the FRA diagram of the transformer. In the proposed method, a three-step optimization algorithm is implemented on the real data of a 33 kV disc winding to find the intensity and occurrence location of faults. At first, the frequency response amplitude signal is decomposed into oscillating modes using successive variational mode decomposition (SVMD), the output of which is much less complicated than the original signal. The frequency response of the modeled circuit decomposition is also obtained in the next stage and in the optimization process, whose decision variables are the RLC values of the detailed (lumped) model of the transformer. Based on the ability to hunt sharks in nature, the new meta-heuristic algorithm of shark smell optimization (SSO) will search for the optimal solution by minimizing the error between the actual and modeled winding frequency response. This process is implemented gradually, with the addition of each oscillatory mode in each stage. The accuracy of the proposed method is evaluated with the data of the tests performed on a 33 kV high voltage disc winding to estimate the parameters of their high frequency electrical equivalent circuit in normal and fault conditions. The results show that the proposed method can estimate the parameters of the equivalent circuit with high accuracy and help to interpret the FRA diagram based on the numerical changes of these parameters.**

***Index Terms* - *Transformer, Frequency Response Analysis, High Frequency Model, Parameters Estimation, Optimization Algorithm***

## I. INTRODUCTION

Transformers are considered the heart of the electrical power system and, therefore, should be carefully monitored to improve system reliability and service continuity. Thus, different diagnostic methods have been established to detect faults within transformers [1]. The dissolved gas analysis (DGA), partial discharge (PD) measurement, thermal analysis (TA), and transformer function assessment are the main diagnostic methods introduced in literature [2]-[4].

Received; 2025-02-03 Revised; 2025-04-15 Accepted; 2025-09-24

[1] Faculty of Electrical and Computer Engineering , Semnan University, Semnan, Iran.
[2] Faculty of Electrical and Computer Engineering , Semnan University, Semnan, Iran.

• Corresponding author Email: zmoravej@semnan.ac.ir

**Cite this article as:**
Jamshidi, S. and Moraveg, Z. (2025) Determining the intensity and occurrence location of faults in transformers using frequency response analysis (FRA) with novel multistage optimization algorithm and SVMD decomposition technique. *Journal of Modeling & Simulation in Electrical & Electronics Engineering (MSEEE), 5*(3), 1-9.

DOI:https://doi.org/10.22075/MSEEE.2025.36778.1200

Among these diagnostic methods, the frequency response analysis (FRA) method has recently been developed and is known to researchers. Therefore, determining faults' location and intensity in the transformer winding has a valuable role in improving future designs and their correction [5], [6]. Recently, several researchers have tried to develop and improve the FRA interpretation process by using new fault detection methods [7]-[10]. The statistical indices are based on the degree of compatibility or lack of compatibility between two sets of fault measurements and the healthy condition of the transformer. Such calculations lead to accurate, objective, and transparent parameters and can also be included in an automatic detection method. The main challenge related to the FRA method is the lack of a systematic and universally accepted interpretation method for test results [11]. A statistical approach can be a helpful tool to overcome this problem. Many research efforts have tried to use different methods and statistical indices to help the process of FRA interpretation [12]. The indices that are usually used are: correlation coefficient, spectrum deviation, and maximum absolute difference of standard deviation, absolute sum of logarithmic error, mean square error, absolute difference, error of ratio of sum of squares, weighted normal difference, T test, and F test [13]-[15]. However, there is no comprehensive comparison study to assess the sensitivity of these numerical indices against different faults in different frequency bands. Consequently, if it is intended to use a numerical index to interpret FRA signatures, it is unknown which one is appropriate.

Previous research in the field of FRA usually has simplifications such as the approximation of the high-frequency equivalent circuit, reducing the number of frequency points, etc., which reduces the accuracy of calculations and does not show the exact location of the fault and its intensity. In this paper, a three-step optimization algorithm is implemented on the real data of a 33 kV high voltage disc winding to find the intensity and occurrence location of faults in transformers.

This paper is organized in the following manner. The parameters optimization methods and the proposed method are discussed in Section II. In section III, to verify the validity of the proposed method, the main idea of this paper has been implemented on a real disk-type high voltage winding sample. The obtained numerical results have been examined and analyzed to determine the location and intensity of the fault in the winding. In section IV, the conclusions and benefits of this paper are discussed, and at the end, the suggested methods for conducting future research are presented.

## II. PARAMETERS OPTIMIZATION METHODS AND THE PROPOSED METHOD

In this section, the tools and steps of forming the proposed algorithm are examined. The main goal is to develop an algorithm to detect all types of faults on the windings of transformers using the FRA technique. By using the proposed method, it is possible to obtain the electrical parameters of the lumped model of the transformer, which itself represents the physical changes in the windings of the transformer. By comparing the parameters obtained in the state when the transformer is healthy with the state after damage has occurred on the winding of the transformer, it is easy to determine the defective part and the intensity of the defect with a very accurate approximation, which will reduce the amount of costs and the duration of the repair. It greatly reduces the defect for the transformer manufacturer and operating companies.

First, the equations and parameters of the lumped model of the transformer are explained. Since the FRA signal is highly non-linear, this issue will result in the over-complexity of the optimization problem and the possibility of its non-convergence. Therefore, this paper uses the new successive variational mode decomposition method to analyze the signal into the oscillatory modes used. In practice, oscillatory modes obtain much more well-behaved signals. Therefore, it leads to the possibility of faster convergence of the optimization problem to find the parameters of the lumped model. In the next section, the meta-heuristic SSO algorithm is described as an algorithm based on the ability of the shark as a top predator in nature to find prey, which is inspired by the shark's sense of smell and its movement towards the odor source. This method has been used to obtain the parameters of the lumped model of the transformer by minimizing the amount of error. Finally, the proposed algorithm, which is a combination of the mentioned selected methods, is described in this paper.

### A. Choosing a suitable transformer winding model

An equivalent electrical model is necessary to analyze the transient and permanent behavior of electrical equipment, including transformers. At high frequencies, the behavior of the winding is very complex, which is why its modeling is also complicated. The lumped model is the best model for checking the changes in the physical structure and insulation of the winding and calculating the voltage at its different points [16]. For modeling, it is assumed that the winding consists of several parts. For each section, we include an RLC circuit model to model the electrical and physical characteristics of that section. In this paper, each section contains a disk. Fig. 1 shows the lumped electrical model of a disk winding equivalent.

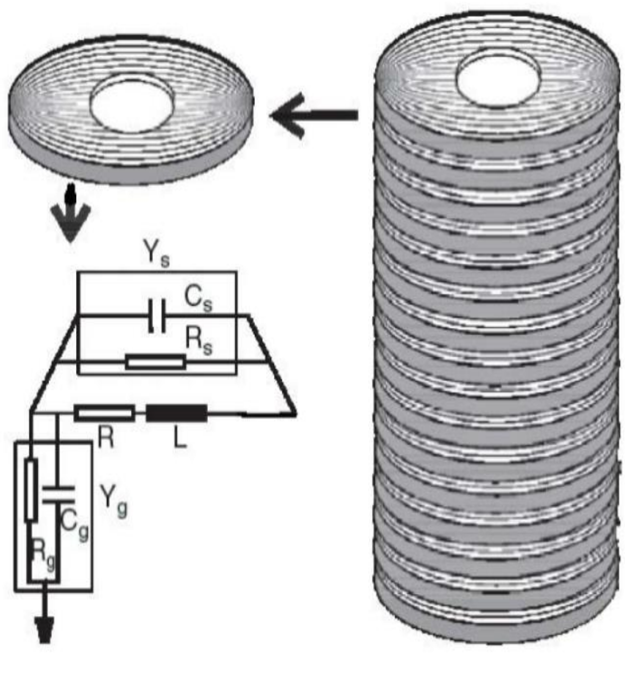


Fig. 1. Transformer disc winding and the model of each disc modeling based on self and mutual inductances.

TABEL I

Definition of Equivalent Circuit Elements

| | |
|---|---|
| $L_i$ | Inductance of each winding section |
| $R_i$ | Ohmic resistance of each winding section |
| $M_{ij}$ | Mutual inductance between the i-th and j-th parts of the winding |
| $C_i$ | Capacitance of each winding section |
| $C_g$ | Capacitance between each section of the winding and the ground or the adjacent winding |
| $R_s$ | Ohmic resistance of the insulation of each winding section |
| $R_g$ | Ohmic resistance of the insulation between each section of the winding and the ground or the adjacent winding |
| $R_E$ | Impedance between the end of the winding and the ground |

To model the high frequency of the transformer winding, we use the circuit equivalent to Fig. 2. The elements shown in this figure are defined in Table I.

By increasing the number of coil sections, the frequency validity limit of its model rises. Because all the parameters depend on the frequency, the model calculations are done in the frequency domain. In this way, the input and output currents of each section and the voltages of all sections are obtained.

*B. Calculation of model parameters*

To solve the circuit of the above model, its parameters must be calculated with the help of mathematical relations, which requires physical information about the winding and insulation properties of the transformer. These parameters are detailed in references [18]-[20]. After introducing the high-frequency model of the transformer winding and calculating its parameters, we must solve this model as a circuit to obtain the current and voltage at different winding points.

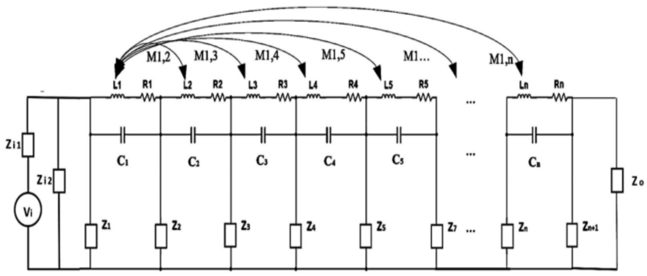


Fig. 2. Lumped model of transformer winding [17].

In this way, we can obtain the transfer function of the transformer between any two arbitrary points. The mathematical description of the model in the frequency domain is usually presented as a matrix of nodal equations using Kirchhoff's first and second laws [18]. In this way, the voltage of all the nodes and the current of all the circuit branches, which are frequency functions, are calculated. The transfer function is obtained by having currents and voltages at different frequencies.

*C. Successive Variational Mode Decomposition (SVMD) technique*

Variable Mode Decomposition (VMD) is a powerful technique for simultaneously decomposing a signal into its constituent intrinsic modes. However, one of the disadvantages of this technique is that it does not accurately determine the number of modes in the signal. In this section, we use a new method called Successive Variational Mode Decomposition [21], which extracts modes sequentially and does not need to know the number of modes. It is also more stable against the initial values of the central frequencies of the modes. The method called variable mode extraction (VME) [22] extracts Intrinsic Mode Functions (IMFs) by knowing their approximate center frequency. In this paper, the extended VME, which is an efficient and fast adaptive method for variable signal decomposition, is used. This new decomposition method sequentially extracts all IMFs (unlike VMD, where the modes are extracted simultaneously). This sequential approach leads to a method without the need to know the number of modes and with less computational complexity compared to VMD. In the SVMD method, decomposition is performed by successively applying VME to the signal, and some restrictions are added to the previously extracted modes to prevent convergence. This method continues until all modes are extracted or the reconstruction error (the error between the input signal and the sum of the modes) is less than a threshold.

In other words, suppose L-1 modes have been found, and you want to determine the next mode. To this end, an optimization problem is solved to find the signal with the maximum compressed spectrum (i.e., the Lth mode) that minimizes the reconstruction error when added to the sum of the extracted modes.

*D. The innovative shark smell optimization (SSO) algorithm*

In this paper, a new meta-heuristic optimization method inspired by the shark hunting ability based on its sense of smell is used, which is called SSO optimization. In this method, different shark behaviors in the search environment, i.e., seawater, are mathematically modeled in the proposed optimization approach [23].

Like other meta-heuristic optimization methods, SSO has several user-defined parameters, including the population size NP and the number of steps $k_{max}$. These parameters can be set separately for each optimization problem. The algorithm can be highly exploratory with large steps in the early stages of evolution and small steps in the last stages (when the algorithm approaches the optimal solution) to benefit from high-resolution search around the optimal solution. After setting parameters, population, and step counter, SSO is initialized. Then the population evolves through forward motion and rotational motion operators. Finally, the best person is selected as the SSO solution for the optimization problem in the last step. The proposed SSO search operators, including gradient-based forward motion and rotational motion-based local search, are specific to this algorithm and are not presented in other meta-heuristic methods.

*E. Algorithm of the proposed model*

Fig. 3 shows the algorithm flowchart of the proposed method to obtain the electrical parameters of the lumped model and to find the location and intensity of the fault.

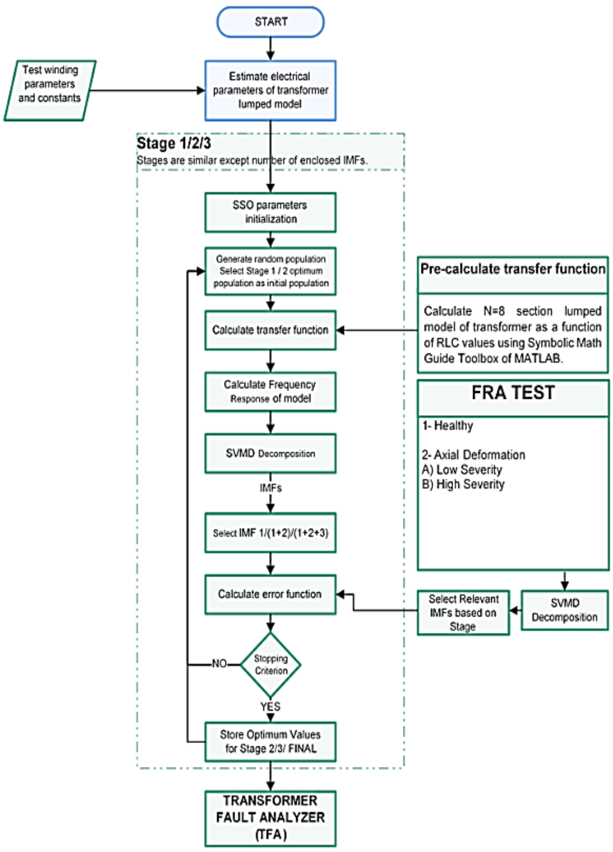


Fig. 3. Algorithm of the proposed method.

### *E.1. Initial estimation of lumped network parameters*

In the proposed algorithm, to perform better in SSO optimization (faster convergence rate) and to limit the range of RLC value changes of the winding lumped network, first, the parameters are estimated using empirical relationships, which are described in reference [18]-[20]. These relationships mainly depend on the physical characteristics of the winding that were measured during the FRA test.

### *E.2. Optimizing SSO, Objective Function calculation process, and using SVMD*

In the proposed algorithm, SSO optimization is used, which is a mathematical model of sharks' movements and behavior in the sea and their hunting environment. This mathematical model is introduced as an optimization method. Looking at the results presented in reference [23], we find that the efficiency and effectiveness of this model for solving real optimization problems are very favorable compared to other meta-heuristic methods.

Looking at the frequency response obtained from the results of the FRA (healthy winding) test, the complexity of the signal shows itself with extreme min and max peaks, which are especially observed at high frequencies. Therefore, we expect the optimization algorithm to reach the desired result with a very large population and many repetitions, which is not desirable from the practical point of view of the fault detection program. The reason for this issue is the hardware limitation, while the goal is for the common hardware to be able to detect the fault in an acceptable period of time. To deal with this issue, the SVMD tool is used, which converts the input signal into several IMF oscillation modes with a limited bandwidth. This transformation identifies important frequencies (center frequencies) with the most frequency content around a limited frequency band and filters the rest of the signal. The great advantage of this transformation is its insensitivity to noise, which shows the superiority of the proposed method. This is because the original signal also contains a high amount of noise due to the nature of the FRA test and faults of unknown origin. Also, using SVMD, another unknown parameter, the number of oscillatory modes, is reduced, which also helps reduce the proposed algorithm's analysis time.

Fig. 5 shows the oscillation modes extracted by SVMD from the frequency response of the tested winding.

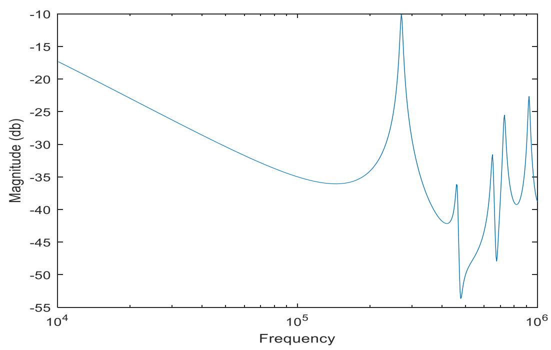


Fig. 4. Frequency response of healthy winding (obtained by FRA test).

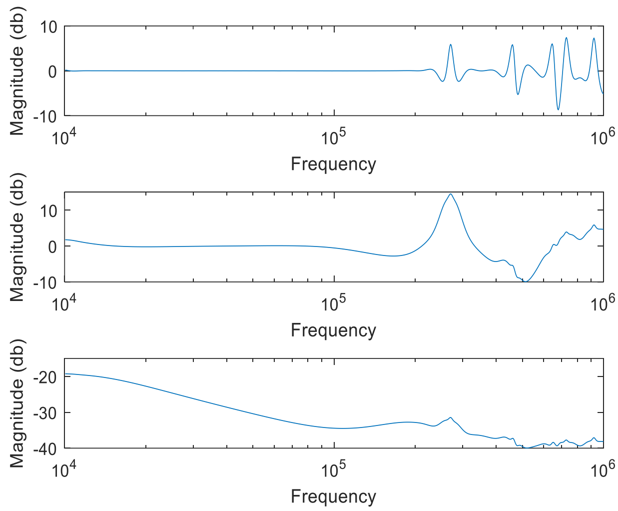


Fig. 5. Extracted oscillatory modes.

As it is known, the number of oscillation modes by the SVMD algorithm is 3. Considering the stability of this number of modes for the tested winding to perform better, the proposed algorithm is designed in three steps. It should be noted that if it is possible for other test windings, the number of oscillation modes extracted by SVMD may increase for any reason. In this case, without losing the generality of the proposed algorithm, only the number of steps will increase to the number of oscillatory modes.

As can be seen in Fig. 5, IMF signals behave much better than the original signal. Therefore, instead of calculating the error of the lumped reconstructed model in each step of the optimization process with the original FRA signal, its error is calculated in the first step with oscillatory mode number 1 (which contains the most frequency content). As shown in section II-D, the sum of IMFs reconstructs the original signal. In the second and third stages, we add the second and third oscillatory modes to the first mode, respectively, to achieve the best possible solutions in the last stage.

In the signal analysis process, the extracted center frequencies are sorted and form IMFs from low to high frequency. Therefore, the algorithm is such that first, the main frequency response error is calculated with the first oscillation mode. Each oscillation mode represents a group of effective RLC parameters, so we expect to get better answers at each stage, which are shown in Section III. The important point is that, as shown in the flowchart of the proposed algorithm in Fig. 5, the optimal response of each stage goes to the next stage as the initial population. This process continues until the final (third) stage, when the final optimal answer is obtained: the RLC values of the described model. It should be noted that the included error is the root mean square of the RMSE error.

For simplicity, the error function of each stage is summarized in Table II.

TABLE II
Error Functions of Each Step

| Step | Error function |
|---|---|
| First | RMSE ( FR , IMF(1) ) |
| Second | RMSE ( FR , ( IMF(1)+IMF(2) ) |
| Third | RMSE ( FR , (IMF(1)+ IMF(2) + IMF(3) ) ) |

The mentioned steps are performed first for the FRA of the healthy winding and then for the winding with axial fault in two degrees, weak and severe, and then the values are compared. In this way, by analyzing the results, you can find out the location of the fault and its intensity. Another item in the proposed algorithm is the pre-calculation section of the lumped model transfer function before the optimization process. One of the most important challenges of using the lumped model of the transformer is the huge amount of time required to perform the related calculations. To deal with this issue in this paper, all calculations are done in matrix form using MATLAB software. Based on the state equations of the expanded circuit given in section II-B, due to the existence of the inverse operator, solving this problem becomes an ill-posed problem from a mathematical point of view, which is the reason why the calculations are time-consuming. Therefore, in this paper, to solve this problem, the transfer function is calculated as a function of RLC values using the Toolbox Symbolic Math Guide, and the optimization algorithm is only called in each iteration. The output of the model obtained using the mentioned method is the transfer function of the lumped model of the transformer, whose parameters are RLC values. Therefore, instead of calculating the transfer function in each iteration of SSO optimization, which will naturally be very time-consuming, only the random values generated by SSO are replaced by the SSO algorithm in the mentioned function, and then the final value of the target function is calculated. Therefore, the volume and calculation time are greatly reduced in the optimization process. The only cost of this work is the long and heavy calculations of equations in the form of parameters, because they are done only once, and are in harmony with the project's goals.

## III. Validation of the Proposed Model and Numerical Results

### *A. Conducting the test on the studied winding in the high voltage laboratory of Arya Transfo Factory*

Fig.s 6 to 8 show the manufacturing stages, calibration, testing, and making faults on the sample tested in this paper. The winding made for this research work has a voltage of 33 kV, contains 64 disks, and each disk contains six turns. The dimensions of the used wire are 7.8 x 1.7 mm.

High-voltage winding with output taps is made every eight disks. These taps are installed in different positions to measure the frequency response. Also, to make a displacement fault in the winding, these taps are cut from different points according to the need, and create the possibility of changing the distances between the disks and the displacement.

The Omicron FRANEO 800 SFRA device (Fig. 8), the latest device manufactured by Omicron, which has a very high accuracy, was used to obtain the frequency response. All measurements were made with the highest accuracy of the device, i.e., ±0.5dB. The tests have been done end-to-end with 2000 frequency points.

Fig. 6. 33 kV high voltage disc winding made specifically for this project.

Fig. 7. Creation of axial displacement fault (axial deformation) on the studied winding.

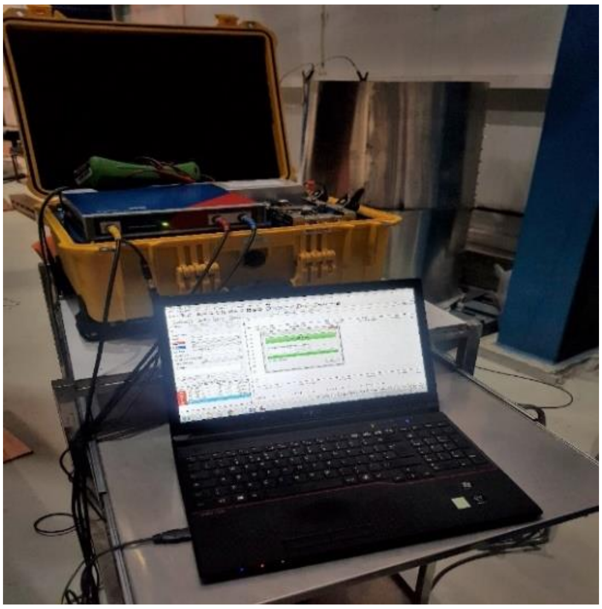

Fig. 8. Calibration of the device and setting the desired values to perform the FRA test.

TABLE III
Specifications of the Winding Made for the Research work of this Paper.

| | |
|---|---|
| Winding Voltage | 33kV |
| Model | Disc Type (High Voltage) |
| Section | 8 |
| Disk per Section | 8 |
| Turn per Disk | 6 |
| Winding Internal Diameter | 43 cm |
| Winding Height | 110 cm |
| Wire Dimension | 1.7 × 7.8 mm (Height × Width) |
| Insulator Dimension | 4 mm (Height) |

### *B. numerical results*

The results obtained from the model estimation algorithm to determine the exact parameters of the transformer windings lumped model are reviewed in the first part of this section. Then the results of the model estimation algorithm are entered into the fault finding algorithm to identify the intensity and location of the fault. As shown in Table III, the number of physical winding sections under study is 8. On the other hand, in the proposed algorithm, the number of sections of the lumped model should be considered to perform pre-calculation and form the parametric transfer function of the winding. It is clear that with the increase in the number of sections in the described model, the accuracy of the model also increases, because RLC parameters specific to each section are considered, and the resulting model will better model the winding behavior. For example, if we assume 16 sections for the lumped model, two sets of parameters are considered for each physical section in the actual winding. On the other hand, the excessive increase in the number of sections of the lumped model causes a sharp rise in the number of parameters of the optimized problem and makes its convergence practically impossible. Therefore, to maintain the model's accuracy and the amount of acceptable calculations in the pre-calculation stage, eight sections have been considered in the lumped model. The average execution time of the algorithm with SSO settings of 50 population, 200 iterations of the first stage, 300 iterations of the second stage, and 500 iterations of the third stage is 45 minutes, which was executed on a PC with a Core i7 processor and 16GB of RAM. The results of the final fitted IMFs of the third stage and the final SFR of the healthy winding are shown in Fig.s 9 and 11. As it is known, the proposed algorithm has approximated IMFs No. 1 and 2 with excellent accuracy. IMF number 3 is an oscillatory mode with a value only at frequencies above 200 kHz, and its amplitude is much lower than that of oscillatory modes 1 and 2 (only 10% of the frequency content compared to the sum of IMF1 and IMF2). The significant difference in some extreme points in this fashion can be analyzed from two aspects. On the one hand, high-frequency fluctuations are mostly noise in nature, and part of it is related to the measurement error of the device. On the other hand, the limitation of the number of sections of the lumped model and the inherent error in its modeling compared to the real model cause such a difference. Nevertheless, the numerical results show that the small error in IMF3 has little effect on finding the location and intensity of the fault, and the results are completely predictable according to the fault created.

In Table IV, $C_g$, $C_s$, L, and $M_i$ are parallel and series capacitors and self and mutual inductances, respectively, and the numbers in the first column show the corresponding section number. In these tables, the value of the parameters is obtained from column 1 and their type from row 1. For example, the value of $C_{g5}$ of the parallel capacitor of section 5 equals 5.23pF. To obtain the value of mutual inductances, both the first column and the first row show the corresponding number of mutual inductances. For example, the value of $M_{3,5}$ tabulated in column $M_3$ and row 5 is equal to 0.71 mH, and $M_{1,2}$ is equal to 1.29 mH. Determining the intensity and location of the fault is possible only after producing the parameters of the exact model of the windings. At this level, the measured winding SFRs are entered into the defect detector algorithm as defective FRs by deforming the disk space.

Fig.s 11 and 12 show the effect of increasing the distance between the discs of section 1 on the FR modes of the studied winding at 3 and 6 mm levels.

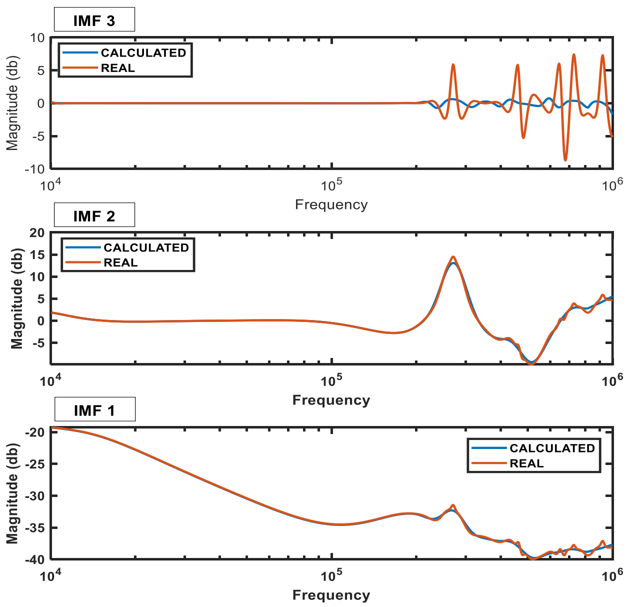


Fig. 9. The results of the final fitted IMFs of the third stage

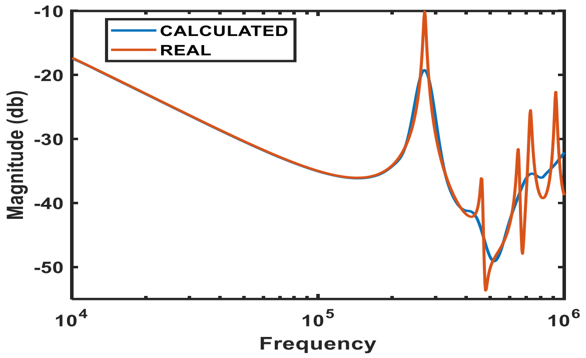


Fig. 10. Frequency response measured by the FRA test and calculated by the optimization algorithm.

TABLE IV
Calculated Parameters of Healthy Winding by Model Estimator.

| Section / Parameter | $C_g$ | $C_s$ | L | $M_1$ | $M_2$ | $M_3$ | $M_4$ | $M_5$ | $M_6$ | $M_7$ |
|---|---|---|---|---|---|---|---|---|---|---|
| 1 | 5.64 | 34.27 | 2.59 | | | | | | | |
| 2 | 5.48 | 35.38 | 2.73 | 1.29 | | | | | | |
| 3 | 5.98 | 31.32 | 2.89 | 0.67 | 1.36 | | | | | |
| 4 | 4.95 | 33.56 | 2.66 | 0.41 | 0.67 | 1.43 | | | | |
| 5 | 5.23 | 33.17 | 2.40 | 0.29 | 0.37 | 0.71 | 1.32 | | | |
| 6 | 5.81 | 32.43 | 2.63 | 0.21 | 0.30 | 0.48 | 0.67 | 1.19 | | |
| 7 | 5.23 | 31.74 | 2.98 | 0.14 | 0.23 | 0.26 | 0.58 | 0.59 | 1.32 | |
| 8 | 5.53 | 32.40 | 2.63 | 0.08 | 0.16 | 0.20 | 0.36 | 0.37 | 0.66 | 1.50 |
| GROUND | 5.65 | | | | | | | | | |

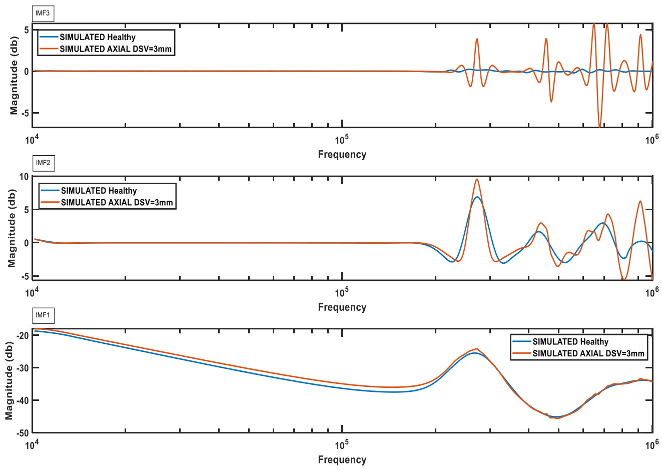


Fig. 11. The effect of increasing the distance between the discs of section 1 on the oscillatory modes of the FR winding - 3 mm.

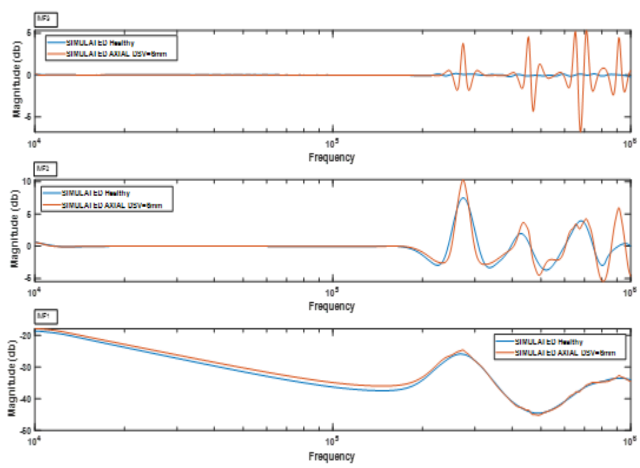


Fig. 12. The effect of increasing the distance between the disks of section 1 on the oscillatory modes of FR winding - 6 mm.

Also, Fig.s 13 and 14 show the effect of the 3 and 6 mm axial DSV disk space deformation fault on the frequency response range, respectively.

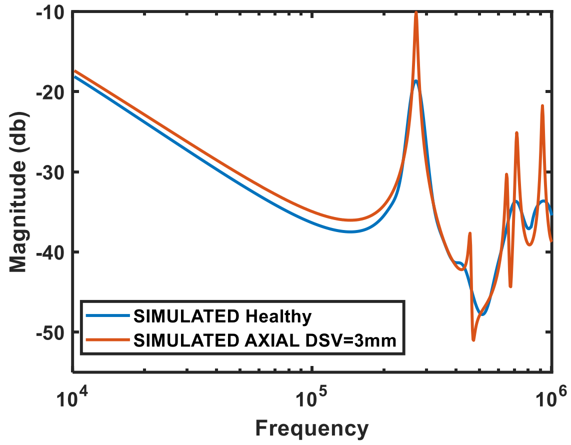


Fig. 13. The effect of increasing the distance between the discs of section 1 on the FR amplitude of the winding at the 3 mm stage.

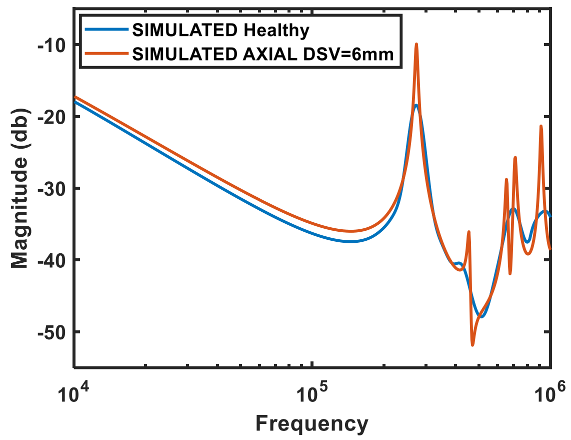


Fig. 14. The effect of increasing the distance between the discs of section 1 on the FR amplitude of the winding at the 6 mm stage.

As shown by the arrow in Fig.s 13 and 14, as the distance between the disks increases, some resonances are gradually moved to the right, and the amplitude of most of them increases. In addition, it can be seen that with the increase of disk space, the changes in the high frequency range of FR increase, and the low frequency range remains more or less unaffected. In the next step, the proposed algorithm of the fault detector program (comparator between healthy and defective windings) receives these two categories of RLC network parameters of the lumped model as deformed windings for further analysis. In both cases, capacitors are identified as dominant groups in the pre-processing stage. The results obtained from the 3 mm DSV in the first part of the fault detector after the last operation in step 2 are presented in Table V. Table VI shows the parameters obtained by the fault detector for a 6 mm DSV in the first section. As can be seen, the fault detector program identified new parameters of all sections with changes compared to the results obtained from the healthy winding. Although the values of most parameters have slight deviations from their values in Table V, some show more changes. For clarification and easier presentation, Tables VII and 8 show the percent change in each parameter from its initial value to better show the effect of shape change on the obtained model.

TABLE V

Calculated Parameters of the Damaged Winding by the Fault Detector in a 3 mm DSV Fault.

| Section / Parameter | $C_g$ | $C_s$ | L | $M_1$ | $M_2$ | $M_3$ | $M_4$ | $M_5$ | $M_6$ | $M_7$ |
|---|---|---|---|---|---|---|---|---|---|---|
| 1 | 5.81 | 24.08 | 2.69 | | | | | | | |
| 2 | 5.74 | 32.68 | 2.83 | 1.34 | | | | | | |
| 3 | 6.03 | 30.38 | 2.96 | 0.67 | 1.42 | | | | | |
| 4 | 4.66 | 34.01 | 2.52 | 0.41 | 0.71 | 1.47 | | | | |
| 5 | 4.98 | 31.89 | 2.29 | 0.31 | 0.36 | 0.74 | 1.29 | | | |
| 6 | 5.71 | 32.24 | 2.52 | 0.22 | 0.32 | 0.50 | 0.63 | 1.15 | | |
| 7 | 5.30 | 30.53 | 3.03 | 0.15 | 0.23 | 0.27 | 0.58 | 0.57 | 1.27 | |
| 8 | 5.79 | 34.24 | 2.75 | 0.07 | 0.15 | 0.18 | 0.35 | 0.37 | 0.64 | 1.50 |
| GROUND | 5.78 | | | | | | | | | |

TABLE VI

Calculated Parameters of the Damaged Winding by the Fault Detector in the 6 mm DSV Fault.

| Section / Parameter | $C_g$ | $C_s$ | L | $M_1$ | $M_2$ | $M_3$ | $M_4$ | $M_5$ | $M_6$ | $M_7$ |
|---|---|---|---|---|---|---|---|---|---|---|
| 1 | 5.57 | 18.91 | 2.58 | | | | | | | |
| 2 | 5.21 | 28.72 | 2.86 | 1.29 | | | | | | |
| 3 | 5.98 | 29.84 | 2.91 | 0.67 | 1.42 | | | | | |
| 4 | 4.98 | 33.03 | 2.64 | 0.39 | 0.72 | 1.45 | | | | |
| 5 | 5.38 | 32.88 | 2.32 | 0.28 | 0.37 | 0.73 | 1.33 | | | |
| 6 | 5.74 | 32.37 | 2.66 | 0.20 | 0.32 | 0.45 | 0.66 | 1.15 | | |
| 7 | 5.40 | 30.29 | 2.93 | 0.16 | 0.24 | 0.26 | 0.57 | 0.58 | 1.34 | |
| 8 | 5.52 | 32.31 | 2.69 | 0.08 | 0.16 | 0.20 | 0.34 | 0.36 | 0.66 | 1.46 |
| GROUND | 5.50 | | | | | | | | | |

TABLE VII

Percentage Change of Parameters Compared to their Healthy Values in a 3 mm DSV Fault.

| Section / Parameter | $C_g$ | $C_s$ | L | $M_1$ | $M_2$ | $M_3$ | $M_4$ | $M_5$ | $M_6$ | $M_7$ |
|---|---|---|---|---|---|---|---|---|---|---|
| 1 | 3.04 | 29.71 | 3.80 | | | | | | | |
| 2 | 4.89 | 7.64 | 3.60 | 3.89 | | | | | | |
| 3 | 0.72 | 2.99 | 2.40 | 0.92 | 4.56 | | | | | |
| 4 | 5.81 | 1.37 | 5.26 | 1.13 | 5.57 | 2.71 | | | | |
| 5 | 4.79 | 3.87 | 4.26 | 6.72 | 0.81 | 4.33 | 2.63 | | | |
| 6 | 1.68 | 0.59 | 4.37 | 5.68 | 4.07 | 4.07 | 4.92 | 3.39 | | |
| 7 | 1.26 | 3.84 | 1.68 | 1.19 | 2.91 | 2.72 | 0.72 | 4.12 | 3.81 | |
| 8 | 4.67 | 5.68 | 4.43 | 12.50 | 4.43 | 6.98 | 2.21 | 0.04 | 3.24 | 0.26 |
| GROUND | 2.35 | | | | | | | | | |

TABLE VIII

Percentage Change of Parameters Compared to their Healthy Values in a 6 mm DSV Fault.

| Section / Parameter | $C_g$ | $C_s$ | L | $M_1$ | $M_2$ | $M_3$ | $M_4$ | $M_5$ | $M_6$ | $M_7$ |
|---|---|---|---|---|---|---|---|---|---|---|
| 1 | 1.38 | 44.81 | 0.35 | | | | | | | |
| 2 | 4.84 | 18.84 | 4.57 | 0.01 | | | | | | |
| 3 | 0.12 | 4.71 | 0.88 | 0.42 | 4.98 | | | | | |
| 4 | 0.70 | 1.57 | 0.52 | 3.07 | 7.12 | 1.42 | | | | |
| 5 | 2.91 | 0.87 | 3.23 | 0.91 | 0.82 | 2.63 | 0.29 | | | |
| 6 | 1.19 | 0.19 | 1.30 | 3.58 | 6.57 | 5.76 | 0.95 | 2.90 | | |
| 7 | 3.28 | 4.57 | 1.76 | 7.54 | 4.37 | 0.44 | 1.63 | 2.79 | 1.39 | |
| 8 | 0.13 | 0.28 | 2.20 | 4.24 | 0.18 | 3.69 | 5.59 | 1.65 | 0.11 | 2.22 |
| GROUND | 2.71 | | | | | | | | | |

The series capacitors of the first section of the winding where the fault occurred show many changes compared to the healthy state. For example, the intensity of deformation occurred in the displacement fault increased from 29.71% at 3 mm to 44.81% at 6 mm DSV. In determining the intensity of the fault, it can be seen that the algorithm effectively finds the changed parameter and the percentage of its changes. The analysis of the obtained results also shows that the axial displacement of the disks has a dominant effect on the series capacities.

In fact, by detecting a part of the parameter with the most different value, the fault detector locates the fault, which is determined as the first part of the measurement in this case. It can be seen that the fault detector has effectively determined the fault in the windings. The analysis of the obtained results shows that the location and intensity of DSV occurring in different winding parts are determined with high accuracy.

## IV. Conclusion and Future Work

Due to the high costs of de-assembling transformers and their time-consuming nature, the industry needs a fast, powerful, and efficient method to detect the internal defects of transformers, which can play a valuable role in improving the design for the future and modifying them. The current method used in the industry to interpret FRA relies on graphical analysis, which leads to incorrect interpretation. In this method, fault interpretation and analysis depend on the expertise of personnel rather than relying on standard and automatic codes.

This paper presents an artificial intelligence method to estimate the electrical equivalent circuit parameters from the FRA diagram of the transformer. In the proposed method, a three-step optimization algorithm is implemented on the real data of a 33 kV high voltage disc winding to find the location and intensity of the fault. The results show that the proposed method can estimate the parameters of the equivalent circuit with high accuracy and help to interpret the FRA diagram based on the numerical changes of these parameters. The main advantage of this approach is that the physical meaning of the model parameters facilitates the reliable identification of various faults and hence helps to create reliable interpretation codes for the transformer FRA diagram.

The results and benefits of this paper are summarized below:

- Analysis and optimization with new mathematical methods to solve problems.

- Improving the equivalent circuit of the transformer and making it more accurate with a better approximation.

- Including the number of frequency points that increase the model's accuracy.

- The proposed method can estimate the parameters of the transformer high-frequency model from the FRA diagram with high accuracy.

- A significant deviation of a particular parameter from the reference data set or the corresponding parameter in other steps indicates a fault.

- The type of fault can be recognized based on the physical meaning of the model parameter. The fault level can be determined based on the amount of parameter changes from the reference data set.

• The proposed estimation method can facilitate the development of standard and automatic codes to identify and determine the fault from the FRA diagram of the transformer.

• The results of this research are important. This means we troubleshoot without disassembling the transformer, saving time and money.

• The proposed method can be easily implemented in industrial frequency response analysis.

Considering the limitations of this research, it is suggested that the following should be considered as future research:

• Using other mathematical models, such as the transmission line model (MTL) instead of the lumped model.

• Three-winding transformer modeling to increase the efficiency of the proposed methods and the possibility of validating them with existing transformers in the network.

• Using optimization analytical methods to find the RLC network parameters of the transformer winding.

• Mathematical studies to increase the efficiency of transformer winding models to see the effect of the core at low frequencies, which leads to finding faults related to the core.

• More research is needed to accurately relate the percent change in each parameter to the corresponding fault level.

## Conflict of Interests

Professor Zahra Moravej, the corresponding author of this paper, is the Co-Editor-in-Chief of the Journal of Modeling and Simulation in Electrical and Electronics Engineering (MSEEE). Still, she has no involvement in the peer review process to assess this work submitted to the journal. This paper was evaluated, and the Chief Editor of the MSEEE Journal managed the corresponding peer review.

## Acknowledgment

The authors would like to thank the Arya Transfo company for manufacturing the studied windings and providing the high voltage laboratory to perform the tests in this research work.

## References

[1] M. Tahir, S. Tenbholen, and S. Miyazaki, "Analysis of Statistical Methods for Assessment of Power Transformer Frequency Response Measurements," IEEE Trans. Power Del, vol. 36, no. 2, April 2021.

[2] S. Das, A. Paramane, S. Chatterjee," Accurate identification of transformer faults from dissolved gas data using recursive feature elimination method," IEEE Trans. Dielectr. Electr. Insul, pp. 466-473, May 2023.

[3] D. Kashani-Gharavi, R. Faraji-Dana, H. Reza Mirzaei. 'A Machine Learning Based Hybrid Algorithm for Partial Discharge Localization in Power Transformers'. IEEE Transactions on Electromagnetic Compatibility. 2024.

[4] Wani SA, Khan SA, Gupta D, Nezami MM. ''Diagnosis of incipient dominant and boundary faults using composite DGA method''. Int Trans Electr Energ Syst. 2017;27(11).

[5] Raichura Maulik, Chothani Nilesh, and Patel Dharmesh. "Efficient CNN-XG Boost technique for classification of power transformer internal faults against various abnormal conditions." IET Generation, Transmission & Distribution, Vol.15, Issue 5, pp. 972–985, 2021.

[6] J. C. Gonzales and E. E. Mombello, "Fault interpretation algorithm using frequency-response analysis of power transformers," IEEE Trans. Power Del., vol. 31, no. 3, pp. 1034–1042, Jun. 2016.

[7] S Mitra; S Pramanik; Parametric Evaluation for Comprehensive Fault Analysis in an Isolated HV-LV Winding Assembly Using Composite Frequency Response. IEEE Transactions on Power Delivery, 2024.

[8] P Mukherjee; S Kumar Panda. Diagnosing Disk-Space Variation in Transformer Windings Using High-Frequency Inductance Measurement. IEEE Transactions on Power Delivery, 2022.

[9] O. Aljohani and A. Abu-Siada, "Application of Digital Image Processing to Detect Short-Circuit Turns in Power Transformers Using Frequency Response Analysis," IEEE Transactions on Industrial Informatics, vol. 12, pp. 2062-2073, 2017.

[10] Aljohani O, Abu-Siada A. Application of DIP to detect power transformers axial displacement and disk space variation using FRA polar plot signature. ," IEEE Transactions on Industrial Informatics, 2016;13(4):1794-1805.

[11] A. Abu-Siada, M. I. Mosaad, Do Won Kim and Mohamed F. El-Naggar, ''Estimating Power Transformer High Frequency Model Parameters using Frequency Response Analysis''. IEEE Trans. Power Deliv. 2019.

[12] M. Tahir, S. Tenbohlen, and S. Miyazaki, "Analysis of Statistical Methods for Assessment of Power Transformer Frequency Response Measurements," IEEE Transactions on Power Delivery, 2021.

[13] Behjat, V.; Mahvi, M. Statistical Approach for Interpretation of Power Transformers Frequency Response Analysis Results. IET Sci. Meas. Technol. 2015, 9, 367–375.

[14] Behjat, V.; Mahvi, M.; Rahimpour, E. New Statistical Approach to Interpret Power Transformer Frequency Response Analysis: Non-Parametric Statistical Methods. IET Sci. Meas. Technol. 2016, 10, 364–369.

[15] S. Miyazaki, M. Tahir, and S. Tenbohlen, "Detection and quantitative diagnosis of axial displacement of transformer winding by frequency response analysis," IET Gener. Transm. Distrib., vol. 13, no. 15, pp. 3493–3500, Aug. 2019.

[16] A. Shintemirov, W. Tang, and Q. Wu, "Transformer core parameter identification using frequency response analysis," Magnetics, IEEE Transactions on, vol. 46, no. 1, pp. 141 –149, Jan. 2010.

[17] M. Jahan, R. Keypour, H. Izadfar, and M. Keshavarzi, " Locating power transformer fault based on sweep frequency response measurement by a novel multistage approach," IET Science, Measurement & Technology, 2018.

[18] E. Rahimpour, J. Christian, K. Feser, and H. Mohseni, "Transfer function method to diagnose axial displacement and radial deformation of transformer windings," IEEE Transactions on Power Delivery, vol. 18, pp. 493-505, 2003.

[19] Almas Shintemirov, ''Modelling and Condition Assessments of Power Transformers Using Computational Intelligence, PHD thesis, The University of Liverpool, U.K., 2009.

[20] Eilert Bjerkan, ''High frequency modelling of power transformers'' PHD thesis, The Norwegian University of Science and Technology, 2005.

[21] M. Nazari, M. Sakhaei. Successive variational mode decomposition. Elsevier, Signal Processing, 2021.

[22] M. Nazari, S.M. Sakhaei, Variational mode extraction: an efficient method for single-lead ECG-derived respiration, IEEE J. Biomed. Health Inf. 2018.

[23] O. Abednia, N. Amjady, A. Ghasemi, A New Metaheuristic Algorithm Based on Shark Smell Optimization, Wiley. 2014.

## Biographies

**Siavash Jamshidi** was born in Khorramabad in the west of Iran, on March 20, 1992. He graduated from Lorestan University with a B.E. and Semnan University with an M.Sc., both in power electrical engineering. Now, he is studying for PHD in power electrical engineering at Semnan University.

His employment experience included the Arya Transfo Company, Semnan. His special fields of interest included power transformers.

**Zahra Moravej.** She received the B.E. and M.E degrees in electrical engineering from Bangalore University, India, in 1985 and 1991, respectively, and the Ph.D. degree from IIT Banaras Hindu University, India, in 2001. Currently, she is a professor at the Electrical and Computer Engineering Faculty at Semnan University, Semnan, Iran. Her areas of research interest include Smart Grid protection, Integration of Renewable Energy Systems, Power System Protection, Control, and Monitoring Power Quality, Power Systems, and Power Electronics AC/DC Microgrids, High-Voltage Direct Current (HVDC) E...